ISSN 1063-7834, Physics of the Solid State, 2016, Vol. 58, No. 9, pp. 1870–1875. © Pleiades Publishing, Ltd., 2016.
Original Russian Text © N.A. Abdullaev, O.Z. Alekperov, Kh.V. Aligulieva, V.N. Zverev, A.M. Kerimova, N.T. Mamedov, 2016, published in Fizika Tverdogo Tela, 2016, Vol. 58, No. 9, pp. 1806–1811.

SURFACE PHYSICS AND THIN FILMS

Weak Antilocalization in Thin Films of the $Bi_2Te_{2.7}Se_{0.3}$ Solid Solution

N. A. Abdullaev[a], *, O. Z. Alekperov[a], Kh. V. Aligulieva[a], V. N. Zverev[b], A. M. Kerimova[a], and N. T. Mamedov[a]

[a] *Institute of Physics, Azerbaijan Academy of Sciences, pr. H. Javid 33, Baku, AZ1141 Azerbaijan*
[b] *Institute of Solid State Physics, Russian Academy of Sciences, ul. Akademika Ossipyana 2, Chernogolovka, Moscow oblast, 142432 Russia*
** e-mail: abnadir@physics.ab.az*

Received August 4, 2015; in final form, March 20, 2016

Abstract—A technology has been developed for the preparation of thin films of the $Bi_2Te_{2.7}Se_{0.3}$ solid solution through the thermal evaporation in a vacuum using the "hot-wall" method. The high quality of the thin films thus prepared has been confirmed by the X-ray diffraction and Raman scattering data. The electron transport has been investigated over wide ranges of temperatures (1.4–300 K) and magnetic fields (up to 8 T). It has been assumed that the observed weak antilocalization is associated with the dominant contribution from the surface states of a topological insulator. The dephasing length has been estimated.

DOI: 10.1134/S106378341609002X

1. INTRODUCTION

Compounds of the $A_2^{\mathrm{V}}B_3^{\mathrm{VI}}$ group continue to be the focus of attention of researchers for a long time. This interest is caused, on the one hand, by the fact that materials of this group are characterized by relatively high values of the thermoelectric figure of merit $zT \sim 1$ ($zT = S^2\sigma T/\chi$, where S is the Seebeck coefficient, σ is the electrical conductivity, T is the temperature, and χ is the thermal conductivity coefficient) and, on the other hand, by the fact that, in recent years, they have considered as topological insulators [1–4]. Usually, the quantities S, σ, and χ are interrelated. However, according to [5–7], a significant increase in the thermoelectric figure of merit can be achieved in low-dimensional systems based on these materials, in which the above parameters can vary more independently, for example, in a quasi-two-dimensional layered system with quantum wells, in superlattices [5, 6], and in a one-dimensional conductor or a quantum wire [7].

In recent years, the transport of charge carriers in thin films of compounds of the $A_2^{\mathrm{V}}B_3^{\mathrm{VI}}$ group has been intensively investigated. From the point of view of investigating the properties of topological insulators, it seems to be important that the contribution from space-charge carriers to their transport can be significantly decreased in thin films. This is confirmed by the data obtained in recent studies devoted to the transport of charge carriers in Bi_2Te_3 and Bi_2Se_3 thin films grown by molecular-beam epitaxy [8–12]. Furthermore, according to [13], thermoelectric devices based on Bi_2Te_3 and Bi_2Se_3 thin films make it possible to achieve a substantial cooling by 32 K and a heat flow pump up to 700 W/cm^2. A local cooling or heating in these thermoelectric devices occurs approximately 2×10^4 times faster than that in devices based on bulk materials. The use of thin films is also preferred for reasons of miniaturization of the devices based on these crystals.

One of the main objectives of this study was to clarify the question as to the extent to which the topological protection of surface states is retained in thin films that are structurally less perfect than the films grown by molecular-beam epitaxy. The choice of just this $Bi_2Te_{2.7}Se_{0.3}$ composition for our investigations is caused, on the one hand, by the fact that the data available in the literature [14, 15] indicate that, in the system of $Bi_2(Te_{1-x}Se_x)_3$ solid solutions, it has the highest thermoelectric efficiency. On the other hand, it is known that the solid solutions are more structurally disordered than the parent compositions $A_2^{\mathrm{V}}B_3^{\mathrm{VI}}$.

In this paper, we have reported the obtained data on electron transport in thin films of the $Bi_2Te_{2.7}Se_{0.3}$ solid solution, which were prepared by a special technology using a simpler and less expensive method of thermal evaporation in a vacuum.

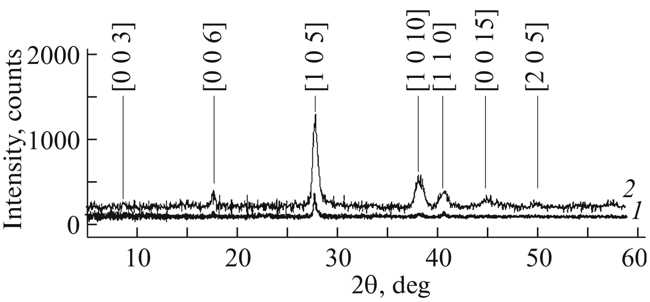

Fig. 1. X-ray diffraction pattern of the (*1*) unannealed and (*2*) annealed $Bi_2Te_{2.7}Se_{0.3}$ films.

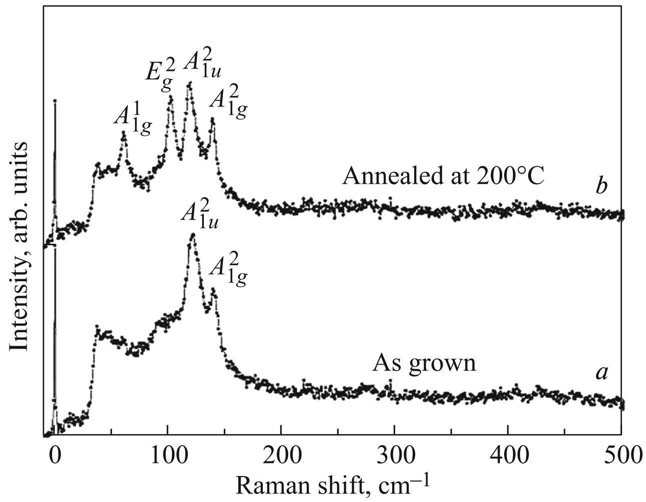

Fig. 2. Raman spectra of the unannealed (curve *a*) and annealed (curve *b*) $Bi_2Te_{2.7}Se_{0.3}$ films.

2. SAMPLES, EXPERIMENTAL TECHNIQUE, AND EXPERIMENTAL RESULTS

The $Bi_2Te_{2.7}Se_{0.3}$ composition was synthesized by melting appropriate amounts of high-purity chemical elements in evacuated quartz ampoules at a temperature of 800°C in a rotary furnace, followed by cooling together with the furnace in the turn-off mode. The films were prepared by the "hot-wall" method through the thermal evaporation of the synthesized substance in a vacuum of 10^{-5} Torr onto oxide silicate glass substrates. The temperature of the substrates was maintained constant at approximately 300°C. The thermal annealing of the prepared films was performed in a vacuum at a temperature of 200°C for one hour. The thickness of the films varied in the range from 500 to 600 nm.

As is known [16], bulk single crystals of bismuth telluride Bi_2Te_3 have a rhombohedral structure with symmetry space group $D_{3d}^5(R\bar{3}m)$. Single crystals of Bi_2Te_3 belong to crystals with a layered structure in which layers are perpendicular to the threefold symmetry axis (the *c* axis). In the structure of the Bi_2Te_3 compound, the layers (or the so-called quintets) consist of five monoatomic hexagonal planes alternating in the sequence Te(1)–Bi–Te(2)–Bi–Te(1).

The structural investigations of the prepared films were carried out on a Bruker D8 Advance X-ray diffractometer. Figure 1 presents the results obtained from the X-ray diffraction investigations, which are typical of the polycrystalline structure, the initial $Bi_2Te_{2.7}Se_{0.3}$ film (curve *1*), and the film annealed in a vacuum at a temperature of 200°C for one hour (curve *2*). It is clearly seen that the annealed film is characterized by a higher intensity of the peaks in the X-ray diffraction patterns (Fig. 1). An improvement in the quality of the films after annealing and an increase in the crystallite size are also indicated by the data obtained from our previous investigations performed on an AIST-NT atomic force microscope (Tokyo Instruments, Japan) [17].

We also studied the Raman spectra of the synthesized thin films of the $Bi_2Te_{2.7}Se_{0.3}$ composition. The spectral investigations were carried out on a three-dimensional confocal Raman microspectrometer Nanofinder 30 (Tokyo Instruments, Japan) at the excitation wavelength $\lambda = 532$ nm. The radiation was detected using a cooled CCD camera (−70°C) operating in the photon-counting mode. The exposure time was 1 min. The frequencies of phonons were determined with an accuracy of 0.5 cm^{-1}. The Raman studies were performed in the backscattering geometry. Figure 2 presents the results obtained from the investigations of the Raman spectra of the unannealed $Bi_2Te_{2.7}Se_{0.3}$ films (curve *a*) and the $Bi_2Te_{2.7}Se_{0.3}$ films annealed at a temperature of 200°C (curve *b*). First of all, it should be noted that the unit cell of the Bi_2Te_3 crystal contains five atoms, and, accordingly, fifteen lattice vibrational modes exist at the center of the Brillouin zone (with $k = 0$), three of which are acoustic and the other twelve are optical. The twelve optical modes are characterized by the symmetry $2E_g + 2A_{1g} + 2E_u + 2A_{1u}$. Each of the modes E_g and A_{1g} is doubly degenerate; i.e., there are four Raman-active and four IR-active modes. According to [18], the four Raman-active modes are characterized by the atomic displacements occurring perpendicular to the *c* axis (the threefold symmetry axis), i.e., in the plane of the layers, in the case of the vibrations E_g^1 and E_g^2 and by the atomic displacements parallel to the *c* axis, i.e., perpendicular to the plane of the layers, in the case of the vibrations A_{1g}^1 and A_{1g}^2.

It can be seen from Fig. 2 that the Raman spectrum of the unannealed film contains two lines at 120 and 138 cm^{-1}, which correspond to the optical modes A_{1u}^2 and A_{1g}^2, respectively. The appearance of the IR mode A_{1u}^2 in the Raman spectrum, apparently, is caused by the symmetry breaking due to the local stresses induced in the film by defects. It should be noted that the A^2_{1u} line is observed in the Raman spectrum not for all parts of the film and is very sensitive to variations in the intensity of the excitation radiation, which also confirms its defective nature. A similar line was observed by Teweldebrhan et al. [19] in the Raman spectrum of ultrathin Bi_2Te_3 films prepared by the mechanical exfoliation. After annealing of the $Bi_2Te_{2.7}Se_{0.3}$ films at a temperature of 200°C, in the Raman spectrum there are additional two lines (at 102 and 60 cm^{-1}) corresponding to the Raman-active modes E^2_g and A^1_{1g} in the bulk crystals [18], which also indicates the crystallization of the films due to the annealing.

Below, we present the results obtained from our investigations of the electrical conductivity, the magnetoresistance, and the Hall effect in the unannealed and annealed samples of the $Bi_2Te_{2.7}Se_{0.3}$ films. The temperature dependences of the electrical resistivity were investigated over a wide temperature range (1.4–300 K) in magnetic fields of up to 8 T. The measurements were performed according to the standard four-probe alternating-current (ac) technique at a frequency of 20.5 Hz by the phase detection method. Point contacts were applied with a silver paste.

Another indication of the crystallization of the $Bi_2Te_{2.7}Se_{0.3}$ thin films after thermal annealing in a vacuum is provided by the data obtained from the investigation of the temperature dependence of the electrical resistivity (Fig. 3). The temperature dependence of the electrical resistivity of the unannealed film (Fig. 3a) exhibits a "semiconductor" character due to the disordered structure. In this case, there is thermally activated hopping conduction through the localized states, which we studied in our previous work [20]. The temperature dependence of the electrical resistivity of the $Bi_2(Te_{0.9}Se_{0.1})_3$ thin film annealed at a temperature of 200°C (Fig. 3b) has a "metallic" character, as is the case in the bulk single crystals [21]: with a decrease in the temperature, the electrical resistivity decreases.

It is an interesting fact that, at low temperatures (below 8 K), a decrease in the temperature leads to a slight increase in the electrical resistivity of the annealed film (Fig. 4). The data obtained from the investigations of the Hall effect at temperatures of 1.4 and 5.0 K indicate that, with a variation in the temperature, the concentration of charge carriers remains unchanged. Thus, the version of the "freezing out" of shallow impurity centers can be excluded. It should be noted that a similar increase in the electrical resistivity with a decrease in the temperature was observed in the low-temperature investigations of different $A_2^{\mathrm{V}}B_3^{\mathrm{VI}}$ thin films grown by molecular-beam epitaxy [8–12]. A similar temperature dependence of the electrical resistivity is characteristic of the case where quantum interference corrections to electrical conductivity due to the weak localization and electron–electron interaction are dominant in the low-temperature range [22]. Since, in the case of a weak localization in an applied transverse magnetic field, a negative magnetoresistance would have to be observed (while in our case, as shown below, there is a positive magnetoresistance), we believe that the observed localization of charge carriers is caused by the electron–electron interaction. The analysis of the temperature dependence of the electrical resistivity at temperatures $T < 8$ K (Fig. 4) revealed that there is a logarithmic dependence of the electrical resistivity on the temperature $\rho(T) \sim \ln T$, which is characteristic of the two-dimensional case [22].

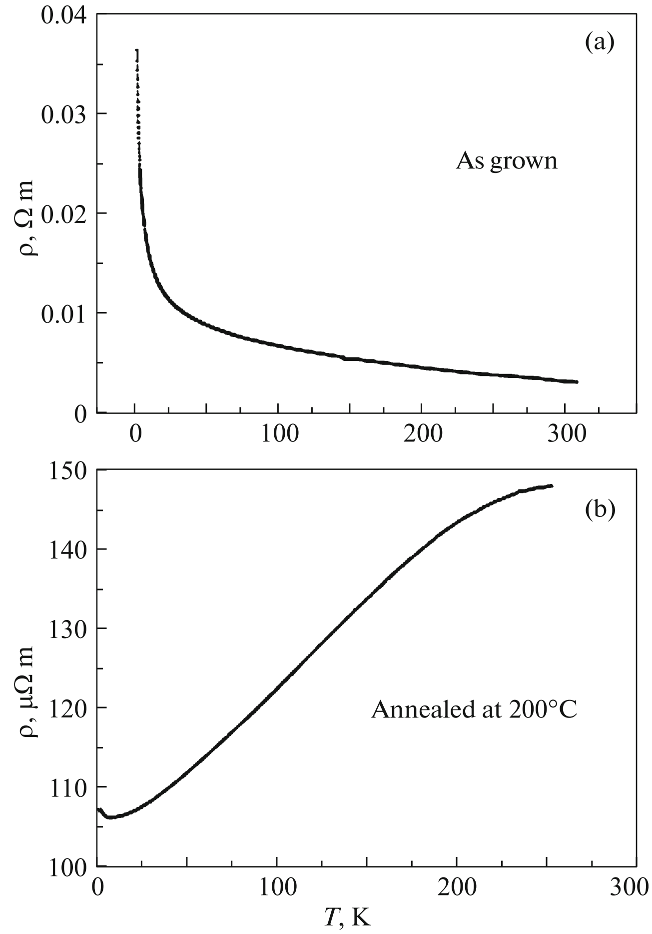

Fig. 3. Temperature dependences of the electrical resistivity of the (a) unannealed and (b) annealed $Bi_2Te_{2.7}Se_{0.3}$ films.

Figure 5 presents the results obtained from the galvanomagnetic investigations of the magnetoresistance (Fig. 5a) and Hall effect (Fig. 5b) in the annealed $Bi_2Te_{2.7}Se_{0.3}$ thin films. From the Hall effect measurements, it follows that the $Bi_2(Te_{0.9}Se_{0.1})_3$ samples have an n-type conductivity. The concentration of electrons in sample no. 1 (for which the data are presented in the

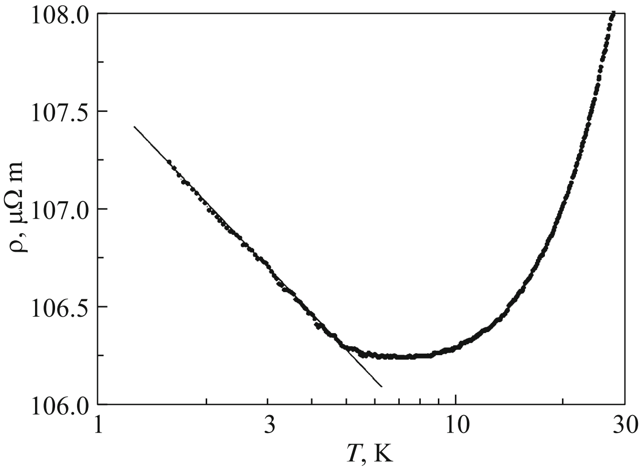

Fig. 4. Temperature dependence of the electrical resistivity of the annealed $Bi_2Te_{2.7}Se_{0.3}$ film at low temperatures.

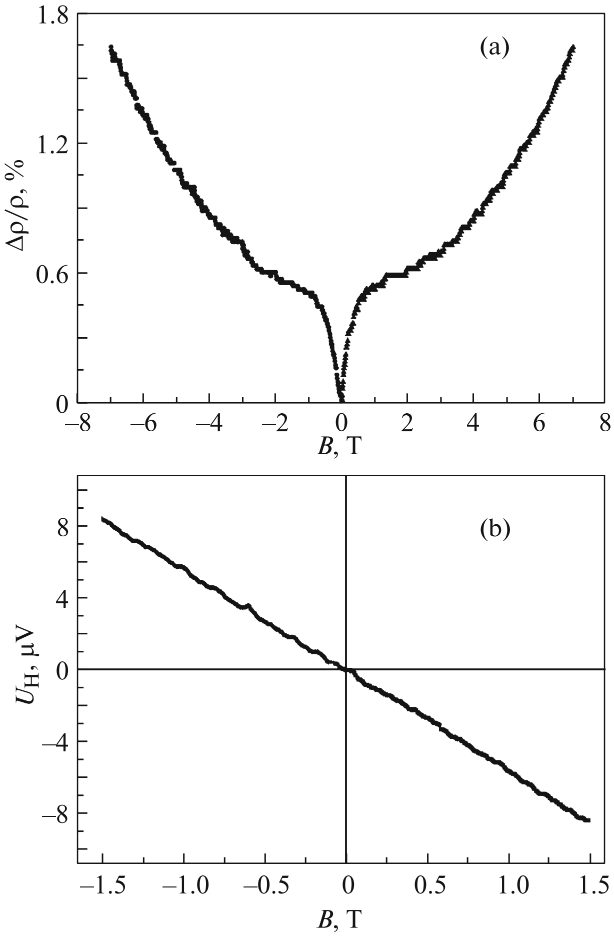

Fig. 5. Results of the investigations of (a) the magnetoresistance and (b) the Hall effect in the annealed $Bi_2Te_{2.7}Se_{0.3}$ thin films.

figures of this paper) is $n \sim 10^{19}$ cm^{-3}, and the Hall mobility of charge carriers μ at a temperature $T \sim 4.2$ K is approximately equal to 100 cm^2/(V s). It should be noted that, at low temperatures, the charge carrier mobility in bulk single crystals is more than one order of magnitude higher than the charge carrier mobility in the annealed thin films: $\mu \sim (3–5) \times 10^3$ cm^2/(V s) [21].

Of particular interest are the results obtained from the field investigations of the magnetoresistance (Fig. 5a). It can be seen from this figure that a sharp increase in the electrical resistivity with an increase of the magnetic field is observed in weak magnetic fields (up to 1 T), whereas in stronger magnetic fields (above 1 T), there is a standard Lorentzian quadratic dependence that is typical of the field dependence of the magnetoresistance in bulk single crystals. Such a sharp increase in the electrical resistivity with an increase of the magnetic field in weak magnetic fields is characteristic of the weak antilocalization effect [22]. The observation of the weak antilocalization effect is not unexpected, because compounds of the $A_2^{\mathrm{V}}B_3^{\mathrm{VI}}$ group are characterized by a strong spin–orbit coupling. However, it should be noted that the weak antilocalization effect is not observed in bulk single crystals, and it is characteristic of only thin films [8–12, 23, 24]. Therefore, it is reasonable to assume that the weak antilocalization observed in thin films is a manifestation of interference effects in near-surface electronic states of a topological insulator.

3. DISCUSSION OF THE RESULTS

An important feature of the surface states of topological insulators is a linear dependence of their energy on the wave vector, which manifests itself in the spectrum in the form of two cones that are in contact at a single point and form the Dirac cone, as is the case in graphene [25]. However, in contrast to graphene, in a topological insulator, for each quasi-momentum on the Dirac cone, there is only one state with a well-defined direction of the spin. It is this feature of the band structure of topological insulators that is responsible for the fact that charge carriers in these spin-polarized states are almost not scattered by surface defects. This is explained by the fact that backscattering of charge carriers in this band by nonmagnetic impurities is symmetry-forbidden with respect to the time reversal. The applied external magnetic field removes the prohibition of the backscattering, which, according to the theory [1, 26], leads to the weak antilocalization effect.

The observed weak antilocalization effect was attributed to the manifestation of the surface states of topological insulators of $A_2^{\mathrm{V}}B_3^{\mathrm{VI}}$ compounds in many previous studies on the transport of charge carriers in a magnetic field, for example, in Bi_2Se_3 thin films [8–11], Bi_2Te_3 thin films [12] and microflakes [23], Sb_2Te_3 nanowires [24], and others. Kim et al. [9]

investigated the dependence of the weak antilocalization effect on the Bi_2Se_3 film thickness that varied by more than three orders of magnitude (from 3 nm to 4 μm). It was shown that the maximum weak antilocalization effect is observed in thin samples and that an increase in the sample thickness leads to a decrease in the weak antilocalization effect. The fact that the weak antilocalization is associated with the dominant contribution from the surface states of a topological insulator is also confirmed by the experiments on the influence exerted by the doping of Bi_2Se_3 thin films with magnetic impurities (Cr) of different concentrations [10]. The energy spectrum of strong topological insulators, including compounds of the $A_2^{V}B_3^{VI}$ group, is topologically protected from disturbances that do not break the symmetry with respect to the time reversal, for example, with respect to the nonmagnetic disorder. The introduction of magnetic impurities breaks the symmetry with respect to the time reversal, which, eventually, with an increase in the concentration of magnetic impurities, leads to the crossover from weak antilocalization to weak localization. He et al. [12] showed that the doping of Bi_2Te_3 thin films with gold nonmagnetic impurities does not affect the weak antilocalization. However, the doping of these films with iron magnetic impurities of different concentrations leads to a gradual disappearance of the weak antilocalization. In addition, the data obtained in [12] from the investigation of the angular dependence of the magnetic conductivity revealed a two-dimensional character of the weak antilocalization effect. Thus, there is good reason to believe that the observation of the weak antilocalization effect indicates the dominant contribution from the topological surface states to the electron transport.

Theoretically, the magnetic-field dependence of the magnetoresistance in the case of a strong spin–orbit coupling ($\tau_\phi \gg \tau_{so}, \tau_e$) in the two-dimensional approximation for weak magnetic fields is described by the Hikami–Larkin–Nagaoka formula [27]

$$\Delta\sigma(B) = \frac{1}{2}\frac{e^2}{2\pi^2\hbar}\left[\psi\left(\frac{1}{2}+\frac{B_\phi}{B}\right)-\ln\left(\frac{B_\phi}{B}\right)\right]. \quad (1)$$

Here, τ_{so}, τ_e, and τ_ϕ are the spin–orbit coupling, elastic scattering, and dephasing times, respectively; e is the electron charge; $\hbar$ is the reduced Planck constant; and $B_\varphi = \hbar/4el_\varphi$ is the characteristic magnetic field, where l_φ is the dephasing length.

We fitted the experimental data by the following formula with two fitting parameters (the coefficient A in front of the whole formula (1) and the characteristic magnetic field B_φ):

$$\Delta\sigma(B) = A\frac{1}{2}\frac{e^2}{2\pi^2\hbar}\left[\psi\left(\frac{1}{2}+\frac{B_\phi}{B}\right)-\ln\left(\frac{B_\phi}{B}\right)\right]. \quad (2)$$

The results of the fitting are presented in Fig. 6. As can be seen from this figure, the theoretical curve (dashed line) calculated using formula (2) is in good agreement with the experimental data for the coefficient $A = 1.1$ and the characteristic magnetic field $B_\varphi = 0.004$ T. According to the estimates, the dephasing length is $l_\varphi = 200$ nm. Although this value is comparable to the film thickness $L \sim 500$ nm, it is necessary to take into account the localization depth of the surface states of the topological insulator, i.e., $a < 10$ nm. Therefore, the condition $l_\varphi \gg a$ is strictly satisfied.

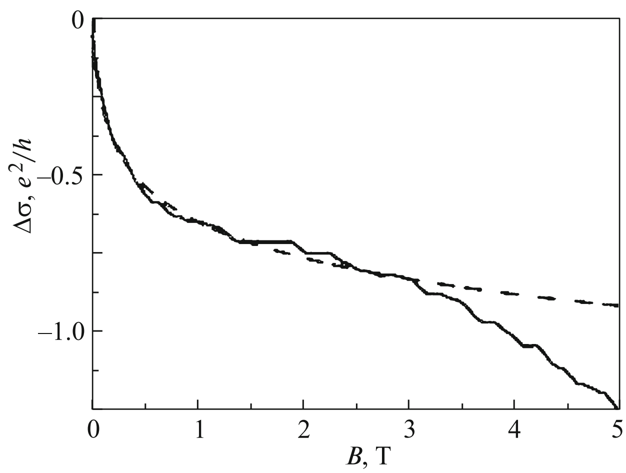

Fig. 6. Field dependence of the magnetic conductivity of the annealed $Bi_2Te_{2.7}Se_{0.3}$ thin films. The dashed line shows the result of the calculation according to formula (2).

The analysis of our experimental data on the temperature and magnetic-field dependences of the electrical resistivity in the annealed $Bi_2(Te_{0.9}Se_{0.1})_3$ thin films revealed an obvious dilemma that was also noted in [8–12, 23, 24]. The negative dip in the magnetic-field dependence of the magnetic conductivity (Fig. 6) is interpreted as the manifestation of topological surface states in the quantum transport. These states have the "immunity" to localization and exhibit a weak antilocalization. However, the measured electrical resistivity increases logarithmically with a decrease in the temperature (Fig. 4), which is characteristic of localization effects in conventional disordered metals [22].

Lu and Shen [28] presented the formula for the electrical conductivity of massless and massive Dirac fermions as a function of the magnetic field and temperature with the simultaneous inclusion of both the electron–electron interaction and quantum interference. This formula eliminates the aforementioned dilemma and shows that the temperature dependence of the electrical conductivity at low temperatures is dominated by the electron–electron interaction, and the magnetic conductivity is determined primarily by the quantum interference due to the spin–orbit coupling. For the experimental verification of the localization of electrons in the low-temperature transport, we propose to perform the investigations using tunneling microscopy at low temperatures.

4. CONCLUSIONS

Thus, in this study, it was shown that the thermal annealing performed in a vacuum at a temperature of 200°C leads to a strong crystallization of the $Bi_2(Te_{0.9}Se_{0.1})_3$ thin films, which was confirmed by the X-ray diffraction and Raman scattering data. The temperature dependence of the electrical resistivity of the annealed $Bi_2(Te_{0.9}Se_{0.1})_3$ thin films exhibits a "metallic" character similar to that observed in the bulk single crystals, but with significant differences in the low-temperature range.

It was found that the logarithmic increase in the electrical resistivity with a decrease in the temperature at temperatures below 8 K is associated with the dominant contribution from the electron–electron scattering to the low-temperature electron transport.

The sharp increase in the magnetoresistance observed at low temperatures (T = 5 K) with an increase of the magnetic field strength in weak magnetic fields (up to 1 T) is caused by the weak antilocalization effect, which is characteristic of the systems with a strong spin–orbit coupling. The observation of the weak antilocalization indicates that the topological surface states dominate in the electron transport in magnetic fields at low temperatures.

In our opinion, the important is the fact that topologically protected surface states persist in the thin films studied in the present work, which are structurally less perfect than the films grown by molecular-beam epitaxy.

ACKNOWLEDGMENTS

We would like to thank S.I. Dorozhkin for helpful discussions.

The study was supported by the Science Development Foundation under the President of the Republic of Azerbaijan (grant no. EIF-2012-2(6)-39/01/1).

REFERENCES

1. L. Fu and C. L. Kane, Phys. Rev. B: Condens. Matter **76**, 045302 (2007).
2. M. Z. Hasan and C. L. Kane, Rev. Mod. Phys. **82**, 3045 (2010).
3. X. L. Qi and S. C. Zhang, Phys. Today **63**, 33 (2010).
4. J. E. Moore, Nature (London) **464**, 194 (2010).
5. L. D. Hicks and M. S. Dresselhaus, Phys. Rev. B: Condens. Matter **47**, 12727 (1993).
6. L. D. Hicks, T. C. Harman, and M. S. Dresselhaus, Appl. Phys. Lett. **63**, 3230 (1993).
7. L. D. Hicks and M. S. Dresselhaus, Phys. Rev. B: Condens. Matter **47**, 16631 (1993).
8. J. Chen, H. J. Qin, F. Yang, J. Liu, T. Guan, F. M. Qu, G. H. Zhang, J. R. Shi, X. C. Xie, C. L. Yang, K. H. Wu, Y. Q. Li, and L. Lu, Phys. Rev. Lett. **105**, 176602 (2010).
9. Y. S. Kim, M. Brahlek, N. Bansal, E. Edrey, G. A. Kapilevich, K. Iida, M. Tanimura, Y. Horibe, S. W. Cheong, and S. Oh, Phys. Rev. B: Condens. Matter **84** (7), 073109 (2011).
10. M. Liu, C. Z. Chang, Z. Zhang, Y. Zhang, W. Ruan, K. He, L. L. Wang, X. Chen, J. F. Jia, S. C. Zhang, Q. K. Xue, X. C. Ma, and Y. Wang, Phys. Rev. B: Condens. Matter **83**, 165440 (2011).
11. Y. Takagaki, B. Jenichen, U. Jahn, M. Ramsteiner, and K.-J. Friedland, Phys. Rev. B: Condens. Matter **85**, 115314 (2012).
12. H.-T. He, G. Wang, T. Zhang, I.-K. Sou, G. K. L. Wong, J.-N. Wang, H.-Z. Lu, S.-Q. Shen, and F.-C. Zhang, Phys. Rev. Lett. **106** (16), 166805 (2011).
13. R. Venkatasubramanian, E. Sivola, T. Colpitts, and B. O'Quinn, Nature (London) **413**, 597 (2001).
14. V. A. Kutasov, L. N. Luk'yanova, and P. P. Konstantinov, Phys. Solid State **42** (11), 2039 (2000).
15. L. V. Prokof'eva, D. A. Pshenai-Severin, P. P. Konstantinov, and A. A. Shabaldin, Semiconductors **43** (8), 973 (2009).
16. B. M. Gol'tsman, V. A. Kudinov, and I. A. Smirnov, *Semiconductor Thermoelectric Materials Based on Bi_2Te_3* (Nauka, Moscow, 1972) [in Russian].
17. N. A. Abdullaev, N. M. Abdullaev, A. M. Kerimova, S. Sh. Kakhramanov, A. I. Bairamov, H. Miyamoto, K. Wakita, N. T. Mamedov, and S. A. Nemov, Semiconductors **46** (9), 1140 (2012).
18. W. Richter, H. Kohler, and C. R. Becker, Phys. Status Solidi B **84**, 619 (1977).
19. D. Teweldebrhan, V. Goyal, and A. A. Balandin. Nano Lett. **10** (4), 1209 (2010).
20. N. A. Abdullaev, N. M. Abdullaev, Kh. V. Aligulieva, A. M. Kerimova, K. M. Mustafaeva, I. T. Mamedova, N. T. Mamedov, S. A. Nemov, and P. O. Bulanchuk, Semiconductors **47** (5), 602 (2013).
21. N. A. Abdullaev, S. Sh. Kakhramanov, T. G. Kerimova, K. M. Mustafaeva, and S. A. Nemov, Semiconductors **43** (2), 145 (2009).
22. A. A. Abrikosov, *Fundamentals of the Theory of Metals* (Nauka, Moscow, 1987; North-Holland, Amsterdam, 1988).
23. S. P. Chiu and J. J. Lin, Phys. Rev. B: Condens. Matter **87**, 035112 (2013).
24. B. Hamdou, J. Gooth, A. Dorn, E. Pippel, and K. Nielsch. Appl. Phys. Lett. **102**, 223110 (2013).
25. A. H. Castro Neto, F. Guinea, N. M. R. Peres, K. S. Novoselov, and A. K. Geim, Rev. Mod. Phys. **81**, 109 (2009).
26. G. Bergmann, Phys. Rep. **107**, 1 (1984).
27. S. Hikami, A. I. Larkin, and Y. Nagaoka, Prog. Theor. Phys. **63**, 707 (1980).
28. H.-Z. Lu and S.-Q. Shen, Phys. Rev. Lett. **112** (14), 146601 (2014).

Translated by O. Borovik-Romanova